International Journal of Applied Earth Observation and Geoinformation 39 (2015) 56–64

Contents lists available at ScienceDirect

International Journal of Applied Earth Observation and Geoinformation

journal homepage: www.elsevier.com/locate/jag

Dry-season vegetation mass and cover fraction from SWIR1.6 and SWIR2.1 band ratio: Ground-radiometer and MODIS data in the Sahel

L. Kergoat [a,*], P. Hiernaux [a], C. Dardel [a], C. Pierre [a], F. Guichard [b], A. Kalilou [c]

[a] GET (CNRS/IRD/Université de Toulouse), 14 Avenue E. Belin, 31400 Toulouse, France
[b] CNRM-GAME (CNRS/MétéoFrance), 42 Avenue Coriolis, 31057 Toulouse, France
[c] ILRI, ICRISAT Sahelian Centre, B.P. 12404, Niamey, Niger

ARTICLE INFO

Article history:
Received 26 September 2014
Accepted 20 February 2015

Keywords:
SWIR
Vegetation mass
Cover fraction
MODIS
Ground radiometry
Sahel

ABSTRACT

The potential of the short-wave infrared (SWIR) bands to detect dry-season vegetation mass and cover fraction is investigated with ground radiometry and MODIS data, confronted to vegetation data collected in rangeland and cropland sites in the Sahel (Senegal, Niger, Mali). The ratio of the 1.6 and 2.1 μm bands (called STI) acquired with a ground radiometer proved well suited for grassland mass estimation up to 2500 kg/ha with a linear relation ($r^2 = 0.89$). A curvilinear regression is accurate for masses ranging up to 3500 kg/ha. STI proved also well suited to retrieve vegetation cover fraction in crop fields, fallows and rangelands. Such dry-season monitoring, with either ground or satellite data, has important applications for forage, erosion risk and fire risk assessment in semi-arid areas.

1. Introduction

Observing dry-season herbaceous vegetation in semi-arid areas is important for a number of applications: forage monitoring, resource management, fire risk and emissions, and also erosion risk assessment (Marsett et al., 2006; Hagen et al., 2012; Ludwig and Tongway, 1995). Still, satellite survey of dry-season vegetation has received far less attention than green vegetation so far. There is now increasing evidence, though, that current sensors like MODIS have strong capabilities to detect dry vegetation, often referred to as non-photosynthetic vegetation, crops residues, or litter (Guerschman et al., 2009; Hagen et al., 2012; Okin et al., 2013). Spectral bands in the SWIR domain have proved particularly efficient, due to the presence of absorption features of different components of dry vegetation tissues like cellulose, hemicellulose or lignin (Asner and Lobell, 2000; Daughtry, 2001). These features are best detected with high spectral resolution data, for instance with the Cellulose Absorption Index (CAI, Nagler et al., 2003), but Guerschman et al. (2009) showed that MODIS bands 6 (B6, 1.6 μm) and 7 (B7, 2.1 μm) could be combined to match CAI ability to detect dry plant tissues. In the same vein, Jacques et al. (2014, hereafter referred to as J14) showed that MODIS ratio B6/B7, also called the Soil Tillage Index (STI), was strongly related to the mass of dry vegetation in Sahelian grasslands.

Using a sensor like MODIS is appealing, since it has a very good temporal resolution (daily time-step) and global coverage. The spatial resolution however is coarse: 500 m at nadir for the SWIR bands. As for other satellite products like Leaf Area Index or Net Primary Productivity, validation and training of algorithms face a scaling issue. Field data are typically collected over a few m^2 for mass, or even less, when pins or lasers are used to estimate vegetation cover fraction (Muir et al., 2011; Nagler et al., 2003). Ground data sampling protocols, in most cases, are tedious and expensive. In the case of the SWIR bands, the situation is particularly complex, since the variables of interest are difficult to measure, even on the ground. For instance, the cover fraction of green vegetation is relatively easily measured using hemispherical or vertical photographs. Conversely, at least over Sahelian bright sandy soils, the contrast between dry vegetation, soil and shadows is weak and the use of classical processing software proved difficult. In the field, it is easier to measure the mass of dry vegetation than its cover fraction. Still, it requires a scaling scheme to be compared with MODIS data.

J14 addressed this issue with an extensive set of 536 satellite-scale mass estimations collected during 8 years over a network of one kilometer long lines in rangelands of Sahelian Mali. They obtained a linear relationship between mass and STI (MODIS B6/B7) characterized by an r^2 of 0.65 and a RMSE of 280 kg of dry matter per hectare (kg DM/ha). This result is potentially very useful for wind erosion risk and forage monitoring applications in the Sahel, and

* Corresponding author. Tel.: +33 561332987; fax: +33 561 33 2888.
E-mail address: laurent.kergoat@get.obs-mip.fr (L. Kergoat).

http://dx.doi.org/10.1016/j.jag.2015.02.011
0303-2434/

probably in other semi-arid grasslands, since it provides a simple method based on easily accessed data. This study raises a number of questions, though. Firstly, there is a significant scatter in the J14 STI-mass relation, which causes have not yet been identified. It might be due to the ground sampling scheme applied to the mass estimation, to the quality of MODIS STI data, or to the variability of target spectral signatures. Any progress in understanding the scatter should lead to improved relationships. Secondly, it would be very valuable to characterize not only pastoral but also agro-pastoral landscapes, consisting in mosaics of crops, fallows and rangelands, especially for erosion risk assessment. Thirdly, it is necessary to investigate the respective importance of vegetation mass and cover fraction in driving STI variability over different dry vegetation canopies.

The objectives of the present study are to document these three questions using MODIS data together with ground radiometry in the 1.6 and 2.1 μm SWIR bands. The Sahelian sites and datasets are presented in Section 2. The results from ground radiometry and MODIS STI, and their relationships with mass and vegetation cover for grasslands, fallow and millet crops are shown in Section 3, and further discussed in Section 4.

2. Sites, data and methods

Data were collected over three Sahelian areas, in Senegal, Mali and Niger (Fig. 1). They consist in ground measurement of vegetation mass and cover fraction, plus ground radiometry in Senegal, together with coinciding MODIS observations, as explained below.

2.1. Vegetation data

In Senegal, data were collected in December 2013 in the Ferlo region. As elsewhere in pastoral Sahel, the vegetation is dominated by annuals grasses and dicots with scattered trees and shrubs. *Aristida mutabilis*, *Schoenfeldia gracilis*, *Eragrostis tremula*, *Dactyloctenium aegyptiacum*, *Chloris prieurii*, *Cenchrus biflorus*, *Alysicarpus ovalifolius*, and *Zornia glochidiata* were the dominant species in the sampled sites. The tree cover was usually within the 0–10% range. Annual rainfall in 2013 was close to normal and ranged from 200 to 350 mm. Herbaceous vegetation mass was measured for groups of 1 m^2 plots or along 500 m lines (Fig. 1). For each plot, dominant species were recorded and vertical pictures were taken for cover fraction estimation. Aboveground vegetation was cut, dried and weighed, with standing and laying parts treated separately.

In the Ferlo rangelands, 500 m lines were sampled over sites belonging to a long-term ecosystem survey (Diouf and Lambin, 2001) and next to two recently installed soil moisture stations. Over each line, the average mass is estimated using a stratified random scheme (Hiernaux et al., 2009 J14). Each 1 m^2 of the line

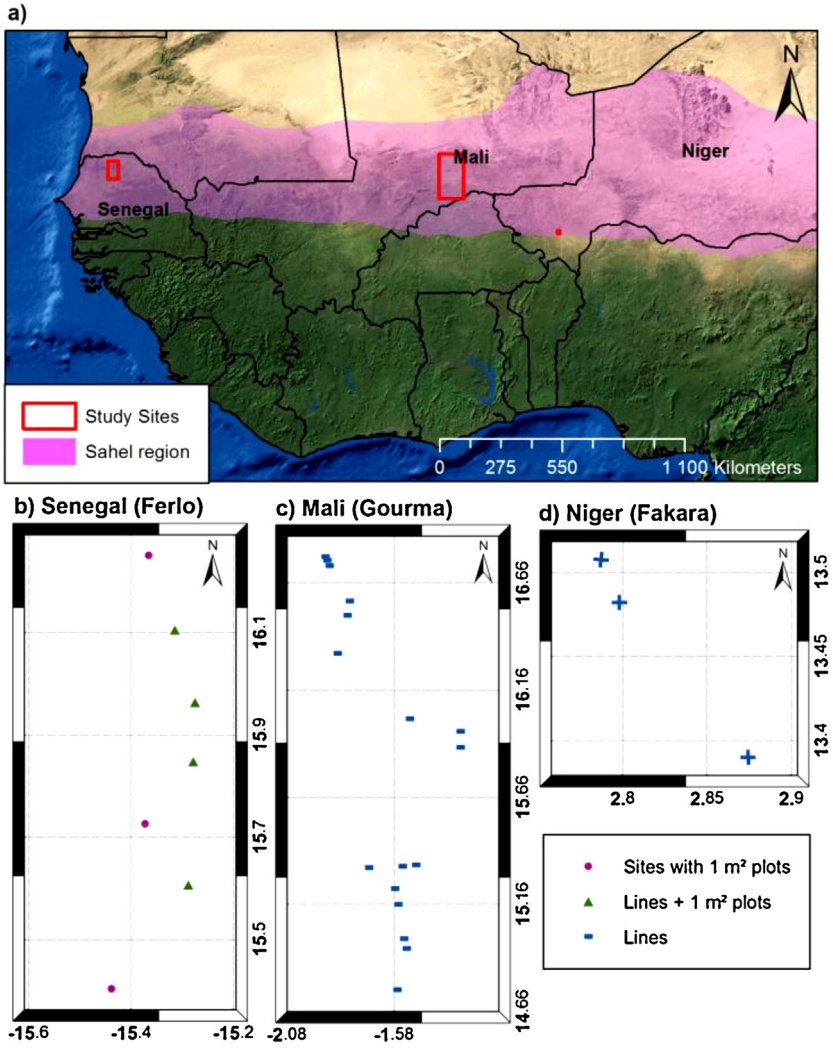

Fig. 1. Location of study sites in the three sahelian countries.

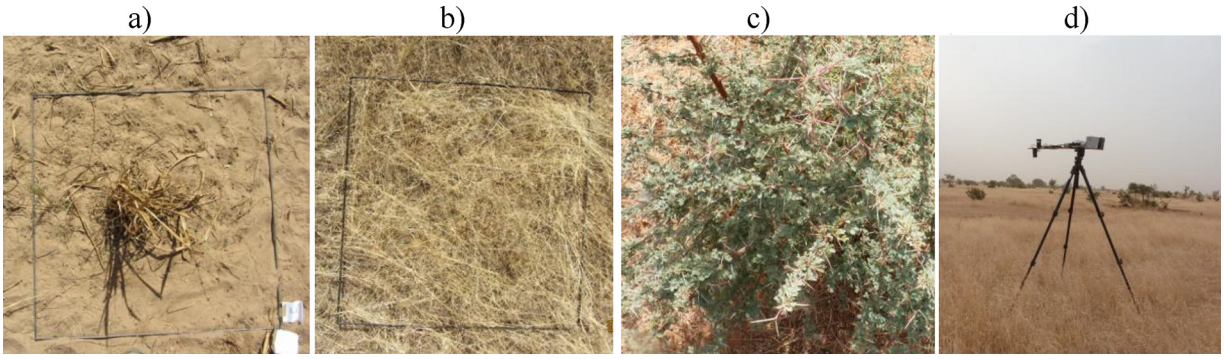

Fig. 2. Plots over millet residues (a), grassland (b), and *Acacia raddiana* bush (c). The dark frame in (a) and (b) delimits a 1 m^2 plot. (d) is the SKYE radiometer fitted on a tripod.

is visually classified into four classes (bare soil and low, medium, high vegetation mass). Each class is characterized by destructive measurements of mass using three 1 m^2 plots per class, randomly selected along the line. The mass estimated for the whole line is the average of the classes masses weighed by their frequency in the line. A total of 97 grassland plots were measured, with the objective of sampling different mass levels and species compositions. Four 1 m^2 plots were also acquired over millet crop residues (Fig. 2a).

Data from Mali also belong to a long-term ecosystem survey (Mougin et al., 2009). A network of 1-km lines has been designed to sample the Sahelian climate gradient, (annual rainfall from 100 to 450 mm), soils types and grazing pressure (Hiernaux et al., 2009), in a grass-dominated ecosystem fairly similar to the Ferlo region. Most of the sites were selected to be homogenous at the 5-km scale and therefore well adapted to MODIS resolution. We use the visual estimates of the vegetation cover fraction that were collected at the one kilometer scale over 2004–2011, using the same stratified random scheme, corresponding to the mass data presented in J14.

By contrast, the sites in southwest Niger are located in a mosaic of crops, fallows and rangelands, where land use is changing from year to year due to crop/fallow rotation (Hiernaux et al., 2009; Dardel et al., 2014a). Three sites were selected to maximize the presence of fallows, millet crops, and fertilized (manured) millet crops within 1 km × 1 km squares, to be consistent with MODIS resolution. The fallow-dominated site was sampled along two perpendicular 1-km lines with the same protocol as in Mali. For crops, stem density and mass per stem were used to compute the crop mass at field scale, and the same sampling as for fallows and pastures was used for weeds. Litter and straws were measured separately. Visual estimates of vegetation cover fraction were also recorded, as well as plant species. The dominant species in 2013 were *Mitracarpus scaber*, *Sida cordifolia* and *Zornia glochidiata* in the fallows, *Pennisetum glaucum*, *Vigna unguiculata* and *Mitracarpus s.* in the crop fields. Rainfall (520 mm) was close to normal. These three sites were measured in October, just after harvest, and then again in December and May. They are noted 'fallow', 'millet' and 'fertilized millet' sites in the following.

The scaling scheme used for all the lines was designed for efficient long-term and large-scale survey compatible with remote sensing. Primary production estimated from the mass dataset provided by this scheme proved remarkably consistent with independent satellite-derived production and precipitation data (Dardel et al., 2014a,b,b). The visual estimations of vegetation cover fraction were mainly performed by the same observer to avoid observer-dependent variability.

2.2. Ground radiometry

The ratio of reflectance at 1.6 and 2.1 μm were measured with a SKYE SKR1820 radiometer (SKYE Instruments Ltd., Powys, UK) during the campaign in Senegal. Incoming radiance is measured with a two-band cosine-response sensor (SKR 1820D), and reflected radiance with a 25° field of view sensor (SKR 1820ND). Bands are centered at 1642 nm and 2135 nm, with bandwidth of 23 nm and 50 nm respectively. The sensors were fitted on a tripod for measures over vegetation plots (Fig. 2) or hand-held for continuous measures over the 500-m lines. Measures were taken every 10 s and logged in a CR1000 data logger (Campbell Scientific, Logan, USA) as 1 min averages. A correction for temperature effects was applied according to the look-up-table provided by the manufacturer. STI was computed as the ratio of the 1642 nm and the 2135 nm reflectance and noted STIg.

The effects of trampling on the radiometric signal (STIg), caused by changes in canopy architecture, were assessed through experimental work. Plots within a homogeneous area were trampled at different intensities, by means of a metal pipe shaped to mimic cattle hoof. STIg was measured before and after trampling, and standing and lying grasses were collected separately. STIg was then measured over bare soil. For each experimental site, one plot was kept untreated, one was fully trampled (all plants lying) and two were trampled at intermediate intensities.

In addition to the continuous hand-held measures along the lines, the twelve 1 m^2 plots used to estimate each line-averaged mass and cover fraction (3 for each class) were measured with the radiometer fitted on the tripod. Therefore, it was possible to compare the line STIg obtained by averaging the continuous measures and the STIg obtained by the weighted-average of the twelve plots as it is done for the mass. Data over *Acacia raddiana* bushes and burned area were also acquired.

2.3. MODIS data

Following Guerschman et al. (2009) and J14, MODIS B6 and B7 reflectance from the Nadir BRDF Adjusted Reflectance (NBAR) product (MCD43A4 collection 5, 500 m resolution) were downloaded along with quality flags. NBAR uses data over a 16-day period to account for BRDF effects and to normalize the reflectance data. STI was computed as the ratio of B6 divided by B7 and noted STIm. Time-series corresponding to the 1-km and 500-m lines were built using only data with the highest quality flag that were interpolated to coincide with field measurements when necessary. Maps are produced from the MCD43C4, collection 5, NBAR product at 5.4 km resolution, combined with the MODIS MCD12C1 land cover

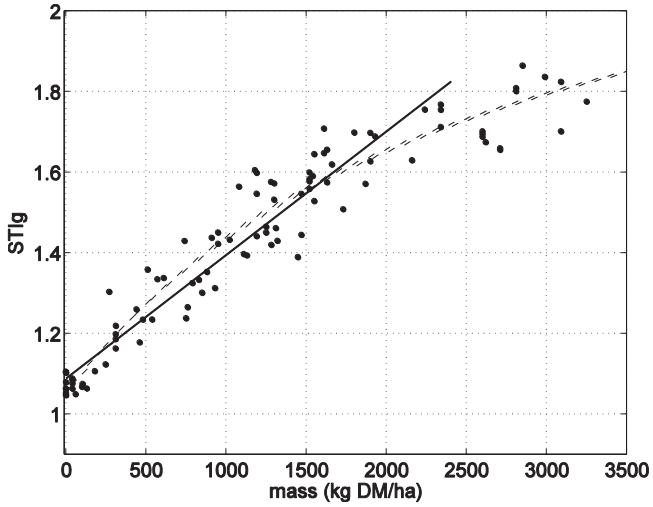

Fig. 3. STIg measured with the SKYE radiometer versus mass, over all grassland plots in Senegal. Full line is a linear fit for mass <2500 kg DM/ha ($r^2 = 0.89$, $n = 84$). Dashed line is a non-linear fit for all data (adjusted $R^2 = 0.93$, $n = 97$).

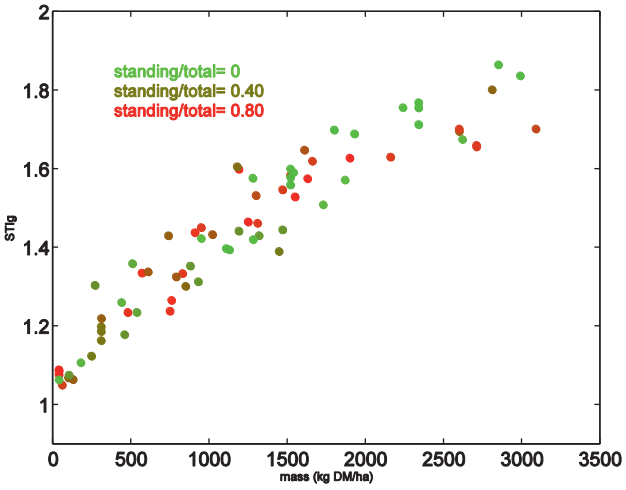

Fig. 4. Effect of canopy architecture on the mass-STIg relation over all grassland plots in Senegal. Color varies from green to red as the ratio of standing to total mass varies from 0 to 1.

map. Pixels with yearly maximum NDVI under 0.11 are masked, so that open water is not mistaken for vegetation.

3. Results

3.1. Ground radiometry

3.1.1. Relationship between ground-based STI and herbaceous mass for grassland

The STIg and herbaceous mass (noted Mass) data obtained with all 1 m^2 plots collected over grasslands in Senegal define a clear relationship (Fig. 3). The mass data range from 0 to 3500 kg DM/ha, and the STIg/mass relationship is fairly linear in the 0–2500 kg DM/ha domain (Eq. (1), $r^2 = 0.89$).

$$\mathrm{STIg} = 1.09 + 3.062\ 10^{-4} \times \mathrm{Mass} \quad (1)$$

STIg values for the 13 mass data larger than 2500 kg DM/ha fall below the linear fit, which implies some saturation of the STIg/mass relation above this threshold. A rectangular hyperbola fits the whole dataset well (Eq. (2), goodness of fit adjusted $R^2 = 0.93$).

$$\mathrm{STIg} = 1.054 + \frac{s \times K \times \mathrm{Mass}}{s \times \mathrm{Mass} + K} \quad (2)$$

With $s = 5.11\ 10^{-4}$ (ha/kg DM) and $K = 1.42$ (unitless). $K + 1.054 = 2.474$ is the asymptotic value of STIg at high masses and s is the slope at Mass = 0.

The mass can be retrieved from STIg, using Eq. (1), for STIg values lower than 1.65, with a RMSE of 198 kg DM/ha. Eq. (2) can be used in inverse mode for the whole STIg range, which yields a RMSE of 300 kg DM/ha. Such precisions make both relations well suited to monitoring applications.

The statistics obtained with ground radiometry and 1 m^2 plots are significantly better than the ones obtained with MODIS and 1-km lines by J14 ($r^2 = 0.65$). The coefficients of the linear relation obtained with ground (here) and MODIS (J14) STI are surprisingly similar, considering that absolute values of ground-based spectral indexes are not expected to match satellite-derived indexes, due to differences in sun-target-sensor geometry, imperfect atmospheric corrections, and calibration for instance.

3.1.2. Effects of canopy architecture and trampling on STI

At the highest mass values, STIg seems to be slightly higher for the lower ratio of standing to total mass (Fig. 4). However, the ratio of standing to total mass does not stand out as a factor explaining the scatter of the STIg-mass relation. Besides, STIg measured after experimental trampling is indeed fairly close to STIg measured before trampling (Fig. 5). Trampling results in similar or slightly smaller STIg values, with an average difference of 0.03. Trampling modifies the canopy architecture in two ways: it leads to a more planophile canopy, which should increase STIg measured at nadir, but it also tends to increase the clumping of the grasses, thus increasing the bare soil fraction. This in turn tends to decrease STIg. Experimental trampling results suggest that the overall effect is weak, and that the clumping effect may be slightly dominant. In natural conditions, trampling is associated with herbivory and aging of the tissues, which are not accounted for during experimental trampling. Nevertheless, these experimental results are consistent with the absence of marked effect of the litter-to-mass ratio on the STIm-mass relation found by J14.

3.1.3. Relationship between STIg and mass estimation over 500-m lines

For each 500-m sampled line, the time-average of continuous 1-min STIg values is close to the weighted-average of STIg of the four classes (twelve 1 m^2 plots) used to estimate the line-average mass

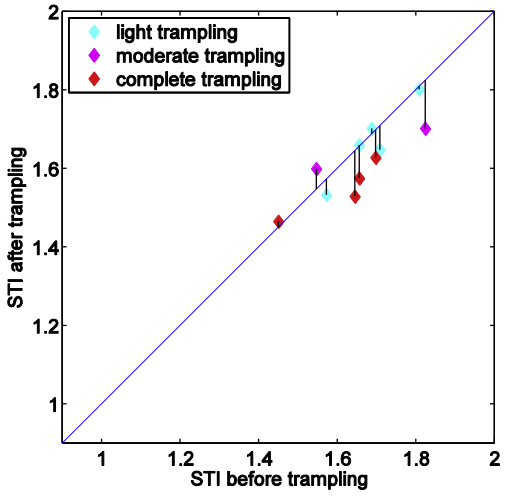

Fig. 5. STIg after versus STIg before experimental trampling, for three levels of trampling.

Table 1
STIg, mass and visual estimation of vegetation cover fraction over four 1 m^2 millet plots, three *Acacia* bushes and a burned area.

	Millet	Millet	Millet	Millet	*Acacia r.* bush	*Acacia r.* bush	*Acacia r.* bush	Burned area
STIg	1.19	1.23	1.14	1.14	2.44	2.22	2.32	1.07
Mass(kg DM/ha)	770	1180	870	880	–	–	–	0
Cover fraction (%)	7	9	6	10	–	–	–	0

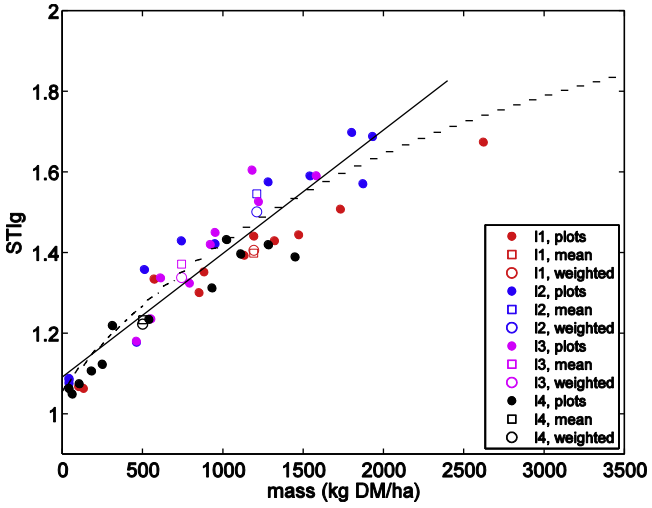

Fig. 6. STIg versus mass for the 1 m^2 plots sampled for each line (full circles), for STIg computed as the weighted-average of the plots (open circles), or as the average of continuous STIg measurements (open squares), versus the line-estimated mass, see Section 3.1.3.
The regression curves of Fig. 3 are redrawn here for comparison.

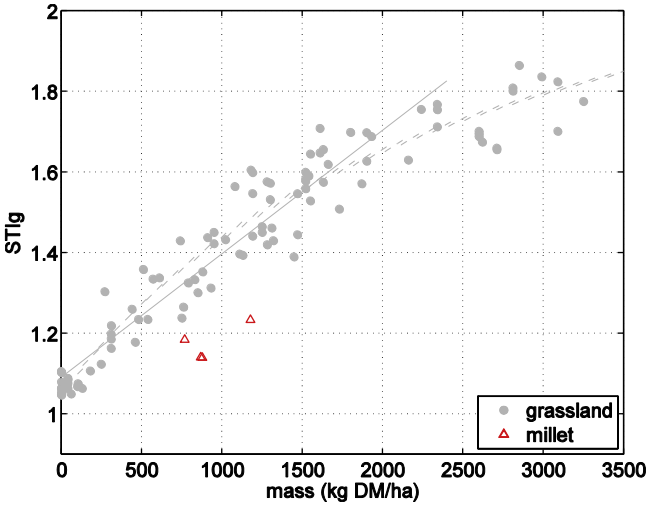

Fig. 7. STIg versus mass for four millet residues plots compared to grassland plots. Two of the four millet plots are almost superimposed.

(Fig. 6). Moreover, the line-scale STIg-mass dots are close to the regressions obtained with 1 m^2 plots (Fig. 3). Although the number of samples is low, these results support the feasibility to use STIg averaged over large lines for monitoring purpose. This is consistent with the linearity of the STIg-mass relation over the 0–2 kg DM/ha range. Additionally, these results point to a good accuracy of the mass sampling scheme.

3.1.4. Signature of bushes, burned area and millet crops

As expected from J14 findings, STIg over the burned area is similar to bare ground STIg (Table 1), and therefore fits to the STIg-mass relations of Fig. 3. Over three small *Acacia* bushes that still had green leaves (Fig. 2c), STIg reaches fairly high values, higher than any STIg

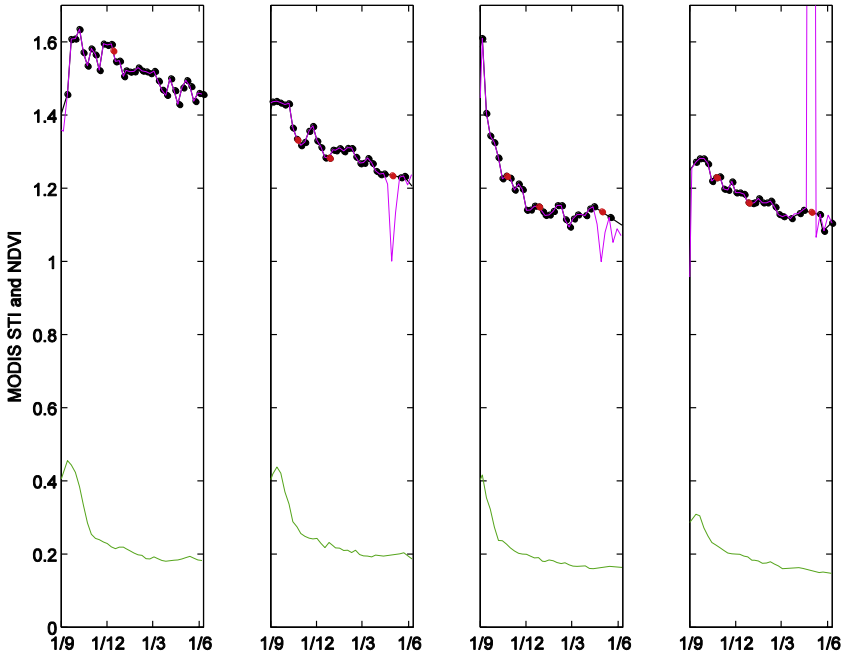

Fig. 8. Time-series of MODIS STI (upper curve) and NDVI (lower green curve) from September 2013 to June 2014. From left to right: Senegal grassland, Niger fallow, Niger fertilized millet and Niger millet sites. The magenta line is the NBAR product, black dots are the NBAR data with highest quality flag, and red dots are the STIm values interpolated to match the date of the field campaigns. The NDVI curves are for highest quality flag NBAR data.

obtained over dry vegetation. In the absence of leaf mass data for these bushes, it is not possible to conclude that these data stand out of the STIg-mass relation, but it is a possibility, which may be due to leaf water content, leaf to mass ratio, or spectral signature of bark, stems or shadows.

Conversely, millet crop residues have lower STIg than predicted by the STIg/mass relationship derived for grassland (Fig. 7). This is in line with a higher fraction of bare soil in millet fields (Fig. 2a). Millet crop residues are highly clumped in the early dry season, since millet is grown in regularly spaced pockets. Clumping decreases during the dry season, as the stems are bent and trampled by cattle. In addition, millet residues also turn from highly erectophile in the early dry season (standing stems and leaves) to more planophile in the late dry season (lying stems and litter). In December, many stems were still standing and highly clumped (Fig. 2a), leading to high mass of tissues despite moderate cover fraction.

3.2. MODIS-derived STI

3.2.1. Time series of MODIS STI over grassland, crops and fallow

Consistently with the results from ground radiometry, STIm computed from MODIS NBAR reflectance over four sites – a grassland site in Senegal, the fallow, millet and fertilized millet sites in Niger – display differences in their seasonal cycles (Fig. 8). The dry-season course of STIm and NDVI for the Senegal grassland site is typical of a non-burned and moderately grazed site, for which STIm decreases much more slowly than NDVI, due to the persistence of significant dry forage. This time-series, as well as the other series over grassland sites in Senegal, matches the ones obtained over grassland in Mali (J14, their Fig. 5). The Niger fallow shares some characteristics with the grassland sites, but the STIm decrease is steeper, and the difference between the STIm and NDVI decrease rates is not as large as for grasslands. The peak STIm over the fallow is also at the lower edge of the STIm over grassland. Over the millet-dominated site, STIm and NDVI peak at lower values also, and then decrease rapidly and similarly, indicating a rapid decrease of plant residues after grain harvest. The fertilized millet site displays large and similar decrease rates of STIm and NDVI during the dry season, but both indexes peak at higher values than for the non fertilized millet crops, just after the rain season (September). Noisy data in late dry season in Niger are efficiently discarded using quality flags. Nevertheless, the STIm series display higher level of noise that NDVI series for all sites.

3.2.2. Mass – STIm relationship over grassland, crops and fallow at MODIS scale

The evolution with time of the total mass of weeds, millet, and herbaceous fallow plants, inferred from the three field campaigns in Niger, is broadly consistent with the time series of STIm: highest values for the fertilized fields in October after harvest, rapid decline of mass for both crop-dominated sites, especially from October to December, and persistence of some dry plants for the fallow site (Table 2)

However, the masses measured over the crop-dominated sites just after harvest stand out of the mass-STIm relationship established for pastoral Sahel by J14, whereas the Senegal grassland sites and the Niger fallow site broadly fit into the same relationship, and therefore extend J14 results to different regions (Fig. 9). Millet high masses are indeed associated with fairly moderate STIm (triangles in Fig. 9).

As such, STIm cannot be used to infer crop residues mass over crop dominated and pasture forage with the same equation, in line with the results obtained with ground-based radiometry. Vegetation mass for grassland and fallow sites in Senegal and Niger, however, can be estimated with Eq. (3) derived from Jacques et al. (2014).

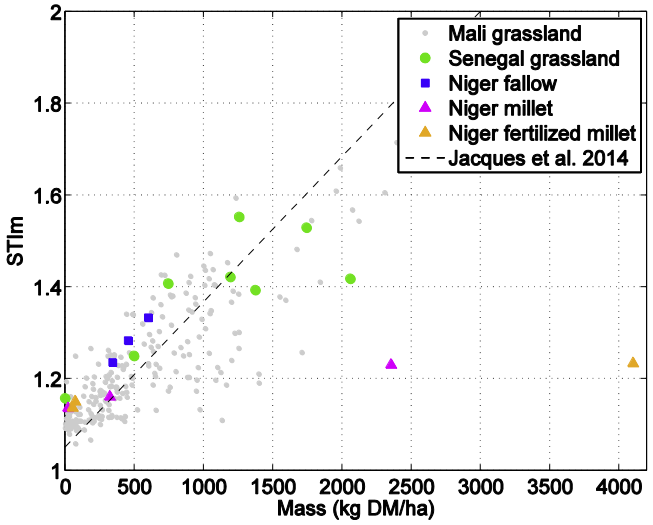

Fig. 9. MODIS STIm versus mass for millet crops and fallow-dominated 1-km sites in Niger, 1-km grassland sites in Mali and 500-m grassland sites in Senegal, together with the linear regression derived by J14 for the Mali sites only.

$$\text{Mass} = 3158 \times (\text{STIm} - 1.05) \quad (3)$$

3.3. Relationship between STI and dry vegetation cover fraction

When cover fraction is used instead of mass, ground-based STIg of the 1 m^2 millet plots comes close to STIg of the grassland plots (Fig. 10). The overall statistics of the relation are less good than for the STIg-mass relationship (Fig. 3), which comes as no surprise since cover fraction is a visual estimate. Non-linearity arises for cover greater than 60%, which suggests difficulties in estimating high cover fraction visually. A linear equation can be derived for cover fraction in the 0–20% range ($r^2 = 0.65$, $n = 36$). When STIg is used, in an inverse mode, to retrieve cover fraction for STIg lesser than 1.5 (Eq. (4)), the RMSE is 4.8%.

$$\text{coverfraction} = 44.5 \times \text{STIg} - 46.26 \quad (4)$$

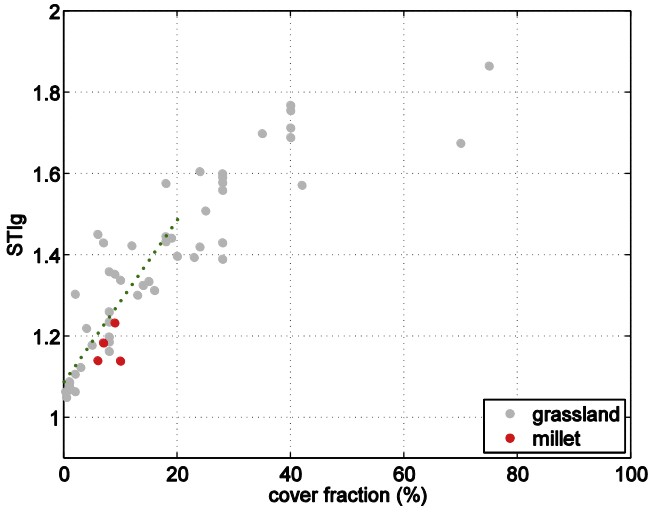

Fig. 10. STIg versus vegetation cover fraction visually estimated for grassland and millet residues in Senegal. The dashed line is the linear regression for cover fractions <20% ($r^2 = 0.65$, $n = 36$).

Table 2
Weeds and millet dry mass and cover fraction over the 1-km lines for the three sites in Niger.

Site	Date	Grass/weeds (kg DM/ha)	Millet stem (kg DM/ha)	Millet leaves (kg DM/ha)	Total mass (kg DM/ha)	Cover fraction (%)
Fallow	25/10/2013	601.2	0.0	0.0	601.2	10.7
Fallow	28/12/2013	429.0	11.3	15.3	455.6	13.5
Fallow	02/05/2014	340.4	2.9	0.8	344.2	5.3
Fertilized millet	27/10/2013	206.5	2446.3	1450.3	4102.1	17.6
Fertilized millet	29/12/2013	11.4	40.0	21.4	72.7	9.6
Fertilized millet	01/05/2014	4.8	40.9	8.3	54	2.9
Millet	26/10/2013	331.4	1139.8	883.2	2353.6	15
Millet	27/12/2013	182.5	74.8	66.0	323.3	6
Millet	01/05/2014	12.8	6.1	3.0	21.9	1.7

Since wind erosion is sensitive to low values of residue cover fraction (Pierre et al., 2014a,b,b), such an accuracy is promising for erosion risk assessment. Moreover, the millet and grassland plots seem to obey the same relation. According to these ground radiometry results, dry-season cover fraction may be determined from STI over different types of dry canopies in the Sahel, even the highly clumped ones.

To extend these findings, the cover fraction for the crop and fallow sites in Niger and the grassland sites in Senegal are plotted against MODIS STIm, together with the Mali grassland dataset (Fig. 11). The data for grasslands show a significant scatter that can be attributed, at least partially, to the poor accuracy of visual estimation of the cover fraction, to the spatial scaling, or to the noise of MODIS time series. Nevertheless, the data over the fallow and crop sites superimpose to the cloud formed by the grassland data. This is not a strong test, given the significant scatter, but it is in line with the ground-based results. Moreover, it provides an equation that can be used for low cover fractions, for instance for STIm lesser than 1.5 or cover fractions lesser than 20%, in both cultivated and non-cultivated Sahel (Eq. (5), RMSE = 5.9%, $r^2 = 0.42$, $n = 226$).

$$\text{cover fraction} = 47.58 \times \text{STIm} - 48.37 \quad (5)$$

3.4. Maps of dry season cover fraction and dry vegetation mass.

The decrease of dry vegetation cover fraction during the long Sahelian dry season is illustrated by a series of maps (Fig. 12 left), obtained with Eq. (5), going from early dry season (22 September 2013) to late dry season (2 June 2014), The early dry season displays a well marked latitude gradient, but with slightly higher values in the Western part of Sahel, as it is expected from the Sahelian precipitation pattern. As the dry seasons progresses, the cover fraction decreases rather rapidly, especially for cropland areas. The two late dry-season maps show minimum values of cover fraction, except for the southernmost areas where the monsoon rain season has already started and has triggered new vegetation growth. The maps of dry vegetation, (Fig. 12 right), obtained from Eq. (3) exhibit a parallel evolution. To our knowledge, these are the first maps of dry season biomass derived from satellite observation for the Sahel.

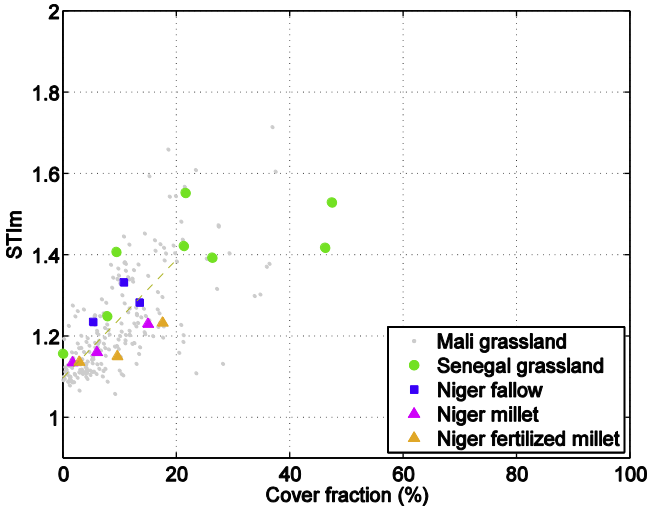

Fig. 11. STIm versus vegetation cover fraction for millet crops and fallow-dominated 1-km sites in Niger, 1-km grassland sites in Mali and 500-m grassland sites in Senegal. The dashed line is the linear regression for STIm <1.5 ($r^2 = 0.42$, $n = 226$).

4. Discussion and conclusion

The quality of the STIg-mass relation obtained here with ground radiometry strongly supports the use of STI for monitoring forage in semi-arid areas. It shows that a linear STI-mass relationship can be used up to 2500 kg DM/ha, and that a curvilinear relation is better suited for masses up to 3500 kg DM/ha. Ground radiometry and MODIS data provide a significant extension of J14, in terms of area (sites in 3 Sahelian countries) and in terms of mass range. It turns out that a simple STI-mass relationship using easily accessed satellite data provides an accurate estimation of forage mass in areas like the Sahel, with relatively bright sandy soils and tree cover commonly around 5%. In areas with contrasted soil brightness and larger tree cover, methods based on end-members (Guerschman et al., 2009; Okin et al., 2013) might be preferred, since trees with green foliage seem to have rather high STI.

The present study shows that better estimations of dry season herbaceous masses over grassland plots are achieved using ground radiometry than using satellite data. Indeed, testing the STI-mass relation with 1 m^2 plots and a ground radiometer alleviates a number of issues. Mass estimation at the MODIS scale requires sampling and scaling. The fact that ground radiometry over the 500-m lines provides a good estimation of the mass gives confidence in the scaling scheme. It is unlikely that errors in line mass estimation are the unique cause of the scatter in the J14 STIm-mass relationship. The noise which affects the STIm time-series is a more probable candidate. Despite the filtering and smoothing caused by the NBAR data processing, STIm time-series are less regular than NDVI time-series. In most cases, no changes in the land surface can explain such a short-term variability in the dry season. In the absence of fire and rainfall, the progressive degradation of the dry grasses is expected to translate into a smooth decreasing time-series. Such a noise was already identified by Lawley et al. (2014), as an issue that impairs the estimation of bare soil fraction with MODIS STI (Guerschman et al., 2009). The STI noise may be due to atmospheric perturbations or sensor signal-to-noise ratio, as well as to occurrence of wetted soils. The latter effect is expected to affect the NBAR product, since it is a change in surface reflectance. However, it is fairly rare in the dry season in the Sahel. It seems that filtering with the quality flags help discarding at least some of rainfall affected data, as they are seen as isolated peaks in a 16-day period and subsequently flagged as outliers. The fact that NDVI seems less affected

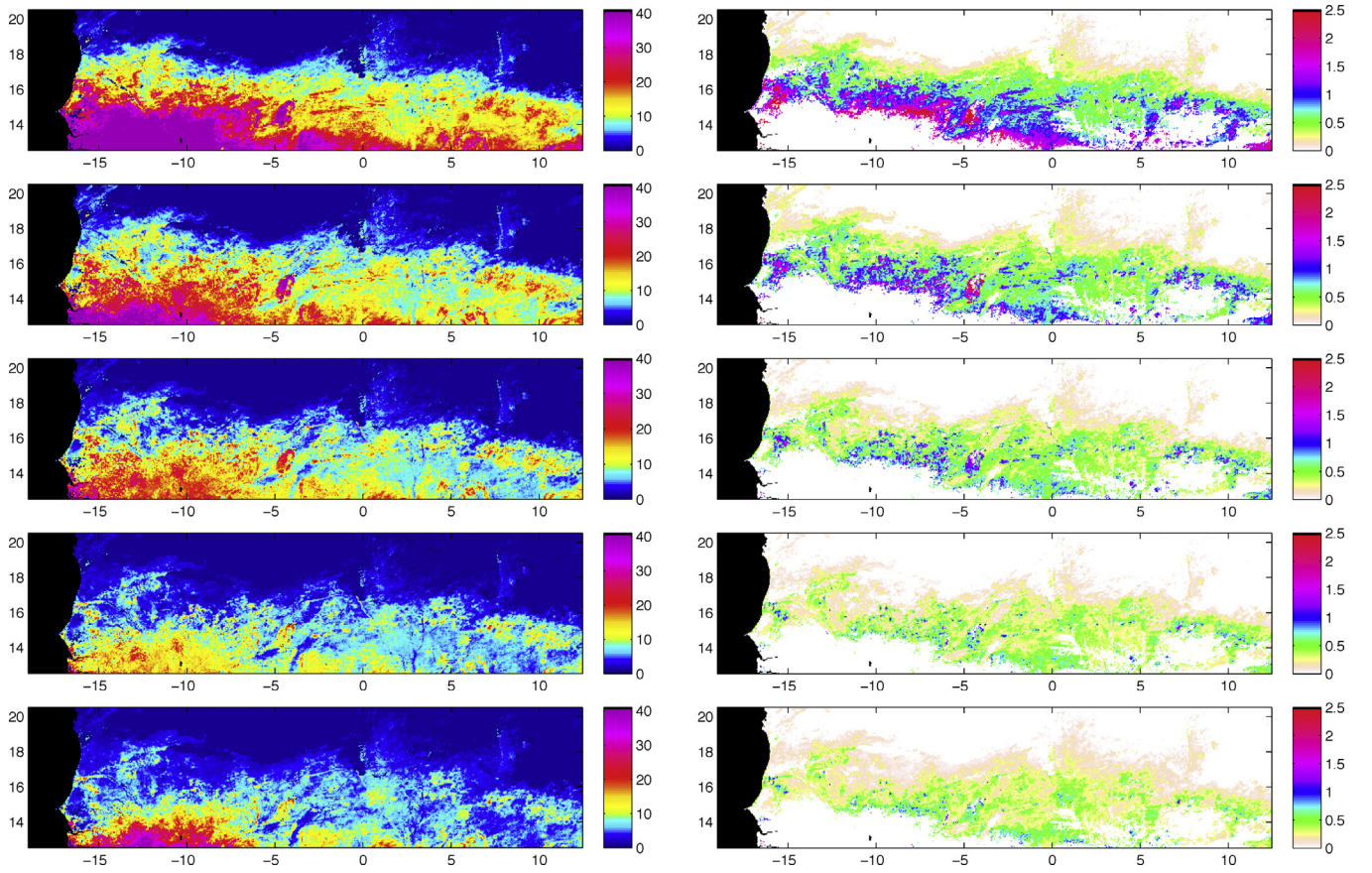

Fig. 12. Evolution of dry vegetation cover fraction (%, left panels) and dry vegetation mass (t DM/ha) along the 2013–2014 dry season. From top to bottom, day periods starting on 22 September 2013, 3 December 2013, 2 February 2014, 14 April 2014, and 2 June 2014. Maps of vegetation mass are restricted to the grassland biome (see text).

than STI by the noise points to a signal-to-noise issue. Indeed, NDVI should be more sensitive to dust loadings than STI. In addition, the SWIR bands have lower signal-to-noise ratio than the VIS and NIR bands, and this has been shown to impact some MODIS products over ocean (Wang and Shi, 2012). Yet the effects of heavy dust loadings on MODIS SWIR bands and STI deserve further investigations. There is room for improving STI, and therefore forage monitoring, if such noise issues can be addressed for MODIS and following sensors. In the meantime, additional smoothing, using curve-fitting for instance, may also improve the MODIS-derived estimations.

Monitoring the mass of residues in crop/fallow mosaic areas was not possible, as opposed to grasslands, at least in the early dry season. This is consistent with the view that STI is primarily sensitive to the vegetation cover fraction, which strongly diverges from mass for highly clumped and erectophile canopy like millet crops and residues. STI might be related to residues mass during the late dry season, when they are mostly litter scattered on the ground. Nevertheless, it seems likely that different STI-mass relationships have to be used when the ratio of mass to cover fraction are different. In terms of protection against erosion, both cover fraction and vegetation mass are relevant. The cover fraction data gathered over different vegetation types, either at the 1 m^2 or 1 km scale, were based on visual estimations, which are far from optimal (Booth et al., 2006). Ground radiometry suggests that the cover fraction over crops and grasslands can be inferred from STI using the same equation. Data at the MODIS scale are consistent with this finding. Further tests with more accurate estimates of bare soil and dry vegetation cover fraction, using "line-point intercept" methods for instance could strengthen these results. Overall, our results show that MODIS-derived STI tracks vegetation cover and bare soil fraction over both pastoral and cultivated Sahel. Given the variety of sites where data have been collected (networks in three different countries), the relationships can be used over Sahel with a good confidence level. It is well possible that they can be used in many semi-arid grasslands worldwide, provided that occasional rainfall periods and dark rocky soils are avoided and best quality flagged data only are retained.

In addition, recently available radiometers like the one used in this study proved to be a convenient device to estimate grassland forage mass, either fitted on a light tripod or hand-held for line measurements. Instrument setup and data processing is fairly simple, and the device is similar to the widely-used field NDVImeters. The high temperature encountered in Senegal did not alter the data, even when it reached the upper range of the temperature look-up table provided for signal corrections (40 °C). Some tests showed that low irradiance and bad sensor leveling should be avoided though. Since the sensors are relatively light, they can be mounted on an unmanned aerial vehicle, which offers promising monitoring methods for remote rangelands.

From a satellite perspective, given that MODIS data are freely available since 2000, and are continued with similar sensors, many applications of STI for mass and dry vegetation cover are conceivable, in the field of forage monitoring, including near real-time monitoring, and in the field of aeolian erosion risk assessment (Pierre et al., 2014a,b,b). Furthermore, dry vegetation cover modulates surface-atmosphere energy and mass exchanges in the dry season (Samain et al., 2008), and vegetation mass and cover also play a role in dryland ecology, as an important resource and habitat for many species in the dry season.

Acknowledgments

Funding from PNTS (PNTS-2012-04), AMMA-CATCH, ANR CAVIARS (ANR-12-SENV-0007-01), CNES and Midi-Pyrénées are acknowledged. We thank N'Diobo Camara (ISE Dakar) and Amadou Kane (IRD Dakar) for their help in Senegal, Idrissa Sane (ISRA Dakar) for access to the Dahra research station, Nogmana Soumaguel, Mamadou Diawara and Eric Mougin for field work in Mali, Laetitia Gal for help with GIS, Damien Jacques for fostering discussions on the STI – mass relation., as well as two anonymous reviewers.

References

Asner, G.P., Lobell, D.B., 2000. A biogeophysical approach for automated SWIR unmixing of soils and vegetation. Remote Sens. Environ. 74, 99–112.

Booth, D.T., Cox, S.E., Meikle, T.W., Fitzgerald, C., 2006. The accuracy of ground-cover measurements. Rangeland Ecol. Manage. 59, 179–188.

Dardel, C., Kergoat, L., Hiernaux, P., Grippa, M., Mougin, E., Ciais, P., N'guyen, C.C., 2014a. Rain-use-efficiency: what it tells us about the conflicting Sahel greening and sahelian paradox. Remote Sens. 6, 3446–3474.

Dardel, C., Kergoat, L., Hiernaux, P., Mougin, E., Grippa, M., Tucker, C.J., 2014b. Re-greening Sahel: 30 years of remote sensing data and field observations (Mali, Niger). Remote Sens. Environ. 140, 350–364.

Daughtry, C.S.T., 2001. Discriminating crop residues from soil by shortwave infrared reflectance. Agron. J. 93, 125–131.

Diouf, A., Lambin, E.F., 2001. Monitoring land-cover changes in semi-arid regions: remote sensing data and field observations in the Ferlo, Senegal. J. Arid Environ. 48, 129–148.

Guerschman, J.P., Hill, M.J., Renzullo, L.J., Barrett, D.J., Marks, A.S., Botha, E.J., 2009. Estimating fractional cover of photosynthetic vegetation: non-photosynthetic vegetation and bare soil in the Australian tropical savanna region upscaling the EO-1Hyperion and MODIS sensors. Remote Sens. Environ. 113, 928–945.

Hagen, S.C., Heilman, P., Marsett, R., Torbick, N., Salas, W., van Ravensway, J., Qi, J., 2012. Mapping total vegetation cover across western rangelands with moderate-resolution imaging spectroradiometer data. Rangeland Ecol. Manage. 65, 456–467.

Hiernaux, P., Mougin, E., Diarra, L., Soumaguel, N., Lavenu, F., Tracol, Y., Diawara, M., 2009. Sahelian rangeland response to changes in rainfall over two decades in the Gourma region, Mali. J. Hydrol. 375, 114–127.

Jacques, D.C., Kergoat, L., Hiernaux, P., Mougin, E., Defourny, P., 2014. Monitoring dry vegetation masses in semi-arid areas with MODIS SWIR bands. Remote Sens. Environ. 153, 40–49.

Lawley, E.F., Lewis, M.M., Ostendorf, B., 2014. Evaluating MODIS soil fractional cover for arid regions, using albedo from high-spatial resolution satellite imagery. Int. J. Remote Sens. 35, 2028–2046.

Ludwig, J.A., Tongway, D.J., 1995. Desertification in Australia: an eye to grass roots and landscapes. Environ. Monit. Assess. 37, 231–237.

Marsett, R.C., Qi, J., Heilman, P., Biedenbender, S.H., Watson, M.C., Amer, S., Weltz, M., Goodrich, D., Marsett, R., 2006. Remote sensing for grassland management in the arid southwest. Rangeland Ecol. Manage. 59, 530–540.

Mougin, E., Hiernaux, P., Kergoat, L., et al., 2009. The AMMA-CATCH Gourma observatory site in Mali: relating climatic variations to changes in vegetation, surface hydrology, fluxes and natural resources. J. Hydrol. 375, 14–33.

Muir, J., Schmidt, M., Tindall, D., Trevithick, R., Scarth, P., Stewart, J.B., 2011. Guidelines for field measurement of fractional ground cover: a technical handbook supporting ground cover monitoring for Australia Canberra: Australian Bureau of Agricultural and Resource Economics and Sciences. http://www.daff.gov.au/abares/publications (accessed 25.09.14.).

Nagler, P.L., Inoue, Y., Glenn, E.P., Russ, A.L., Daughtry, C.S.T., 2003. Cellulose absorption index (CAI) to quantify mixed soil-plant litter scenes. Remote Sens. Environ. 87, 310–325.

Okin, G.S., Clarke, K.D., Lewis, M.M., 2013. Comparison of methods for estimation of absolute vegetation and soil fractional cover using MODIS normalized BRDF-adjusted reflectance data. Remote Sens. Environ. 130, 266–279.

Pierre, C., Bergametti, G., Marticorena, B., Abdourhamane Toure, A., Rajot, J.L., Kergoat, L., 2014a. Modeling wind erosion flux and its seasonality from a cultivated sahelian surface: a case study in Niger. Catena 122, 61–71.

Pierre, C., Bergametti, G., Marticorena, B., Kergoat, L., Mougin, E., Hiernaux, P., 2014b. Comparing drag partition schemes over a herbaceous Sahelian rangeland. J. Geophys. Res. Earth Surf. 119, 2291–2313.

Samain, O., Kergoat, L., Hiernaux, P., Guichard, F., Mougin, E., Timouk, F., Lavenu, F., 2008. Analysis of the in situ and MODIS albedo variability at multiple time-scales in the Sahel. J. Geophys. Res. 113, D14119.

Wang, M., Shi, W., 2012. Sensor noise effects of the SWIR bands on MODIS-Derived ocean color products. IEEE Trans. Geosci. Remote Sens. 50, 3280–3292.